Available online at www.sciencedirect.com
ScienceDirect
Applied Surface Science 253 (2006) 2911–2914
applied surface science
www.elsevier.com/locate/apsusc

Effect of substrate temperature on structure and electrical resistivity of laser-ablated IrO_2 thin films

Chuanbin Wang [a,b], Yansheng Gong [a], Qiang Shen [a], Lianmeng Zhang [a,*]

[a] State Key Laboratory of Advanced Technology for Materials Synthesis and Processing, Wuhan University of Technology, Wuhan 430070, China
[b] Institute for Materials Research, Tohoku University, 2-1-1 Katahira, Aoba-ku, Sendai 980-8577, Japan

Received 7 February 2006; received in revised form 1 June 2006; accepted 6 June 2006
Available online 25 July 2006

Abstract

IrO_2 thin films were prepared on Si(1 0 0) substrates by laser ablation. The effect of substrate temperature (T_{sub}) on the structure (crystal orientation and surface morphology) and property (electrical resistivity) of the laser-ablated IrO_2 thin films was investigated. Well crystallized and single-phase IrO_2 thin films were obtained at T_{sub} = 573–773 K in an oxygen partial pressure of 20 Pa. The preferred orientation of the laser-ablated IrO_2 thin films changed from (2 0 0) to (1 1 0) and (1 0 1) depending on T_{sub}. With the increasing of T_{sub}, both the surface roughness and crystallite size increased. The room-temperature electrical resistivity of IrO_2 thin films decreased with increasing T_{sub}, showing a low value of $(42 \pm 6) \times 10^{-8}$ Ω m at T_{sub} = 773 K.

PACS: 81.15.Fg; 73.50.−h

Keywords: IrO_2 thin films; Laser ablation; Substrate temperature; Structure; Electrical resistivity

1. Introduction

Iridium oxide (IrO_2), as a well-known conductive oxide material, has attractive electrical, optical, and electrochemical properties [1,2]. IrO_2 thin films have also attracted much attention as for ferroelectric devices, diffusion barriers, optical switching layers in electrochromic devices, pH sensors and durable electrode materials for chlorine or oxygen evolution [3,4], etc.

Several film deposition methods have been employed to grow IrO_2 thin films, such as reactive sputtering, sol–gel and laser ablation or pulsed laser deposition [5–9]. Laser ablation is regarded as one of the most effective ways due to its uniformity, reproducibility and simplicity. It was found that properties of the as-deposited thin films were sensitive to or even determined by the structure, while the structure was influenced by deposition parameters especially the substrate temperature (T_{sub}). However, much attention was merely focused on the fabrication process or properties of the laser-ablated IrO_2 thin films. The relationship between the laser ablation parameters and the structure and properties of IrO_2 thin films had been few reported.

In the present study, we successfully prepared highly-conductive IrO_2 thin films by laser ablation. The effect of laser ablation parameter (T_{sub}) on the structure (crystal orientation and surface morphology) and property (electrical resistivity) of the laser-ablated IrO_2 thin films was investigated, so that the desired properties for application could be obtained by controlling the deposition parameters.

2. Experimental procedure

IrO_2 thin films were deposited on Si(1 0 0) substrates by laser ablation. A Q-switch pulsed Nd:YAG laser with a wave length of 355 nm and a repetition frequency of 10 Hz was used. The laser beam was introduced into the chamber at an angle of 45°, and focused on a rotating target at an energy density of 2×10^4 J/m^2. A hot-pressed iridium ceramic pellet was used as the target. The Si(1 0 0) substrates were placed parallel to the target at a distance of 50 mm. The chamber was evacuated to an ultra-high vacuum (8×10^{-7} Pa) and then the laser ablation was carried out under an oxygen partial pressure (P_{O_2}) of 20 Pa for 1 h. The substrate temperature (T_{sub}) was changed from 573 to 773 K.

* Corresponding author. Tel.: +81 22 215 2106; fax: +81 22 215 2107.
E-mail address: wangcb@imr.tohoku.ac.jp (L. Zhang).

0169-4332/$ – see front matter © 2006 Elsevier B.V. All rights reserved.
doi:10.1016/j.apsusc.2006.06.031

The crystal structure of the as-deposited films was examined by X-ray diffractometer with Cu Kα radiation. The Raman shift from a He–Ne laser (633 nm) was measured to further identify the structure of IrO_2 thin films. Atom force microscopy (AFM) was used to measure the surface morphology and roughness of the films. The thickness was observed by scanning electron microscope (SEM), which was found to be about 350 nm. The electrical resistivity of the laser-ablated IrO_2 thin films at room temperature was determined by using the four-point probe method.

3. Results and discussion

3.1. Crystal structure and orientation

Fig. 1 shows the XRD patterns of IrO_2 thin films grown on Si(1 0 0) substrate at $P_{O_2} = 20$ Pa and $T_{sub} = 573$–773 K. All the diffraction peaks could be well indexed to IrO_2 (1 1 0), (1 0 1), (2 0 0), (2 1 1) and (1 1 2), as compared with the standard *d* values taken from JCPDS (43-1019). No other impurity phases except the Si(1 0 0) peaks from the substrate were identified, which indicated that single-phase IrO_2 thin films were obtained at $T_{sub} = 573$–773 K. With the increasing of T_{sub}, the location of IrO_2 diffraction peaks hardly shifted whereas their relative intensity was changed obviously, implying that the preferred orientation of the laser-ablated IrO_2 thin films was different depending on T_{sub}.

The preferential growth orientation could be determined using a texture coefficient, $TC_{(hkl)}$, expressed by the following equation [10]:

$$TC_{(hkl)} = \frac{I_{(hkl)}/I_{0(hkl)}}{1/N\left[\sum I_{(hkl)}/I_{0(hkl)}\right]} \quad (1)$$

Here, $TC_{(hkl)}$ is the texture coefficient of (*hkl*) plane which shows the strongest reflex alone (*hkl*) plane, $I_{(hkl)}$ the measured intensity of (*hkl*) plane, $I_{0(hkl)}$ the corresponding recorded intensity in JCPDS data file, and *N* is the number of preferred orientations.

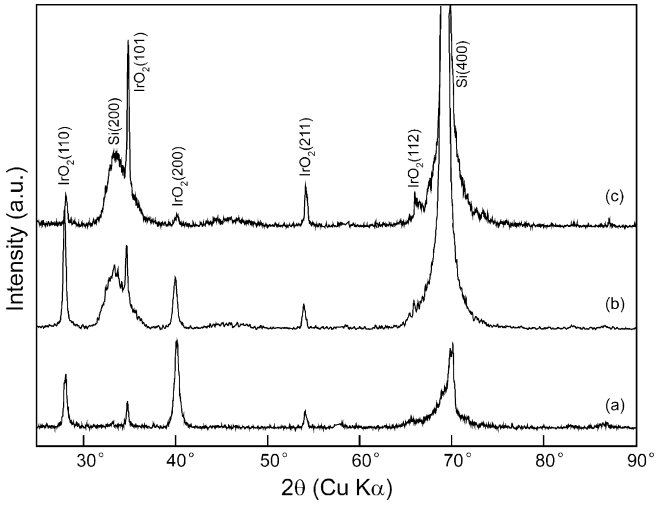

Fig. 1. XRD patterns of IrO_2 thin films grown on Si(1 0 0) substrates at $P_{O_2} = 20$ Pa and (a) $T_{sub} = 573$ K, (b) 673 K and (c) 773 K.

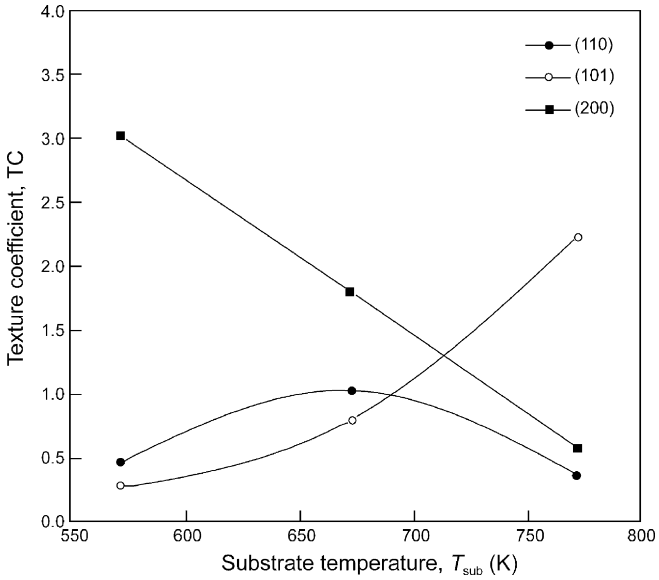

Fig. 2. Variation of texture coefficient $TC_{(1\,1\,0)}$, $TC_{(1\,0\,1)}$ and $TC_{(2\,0\,0)}$ with T_{sub}.

Fig. 2 shows the variation of texture coefficient $TC_{(1\,1\,0)}$, $TC_{(1\,0\,1)}$ and $TC_{(2\,0\,0)}$ of IrO_2 thin films with T_{sub}. From the calculation, it can be seen that $TC_{(2\,0\,0)}$ showed maximum at $T_{sub} = 573$ K, indicating the strongest reflex along (2 0 0) plane comparing with other T_{sub}. Similarly, $TC_{(1\,1\,0)}$ and $TC_{(1\,0\,1)}$ had the maximum value at $T_{sub} = 673$ K and $T_{sub} = 773$ K, respectively. All these indicated that the preferred orientation of the laser-ablated IrO_2 thin films changed from (2 0 0) to (1 1 0) and (1 0 1) with the increasing of T_{sub}.

Raman shift spectra were employed to further identify the crystal structure of IrO_2 thin films deposited at $P_{O_2} = 20$ Pa and $T_{sub} = 573$–773 K, as shown in Fig. 3. The standard peaks characteristic to IrO_2 were located at 561, 728 and 752 cm^{-1}

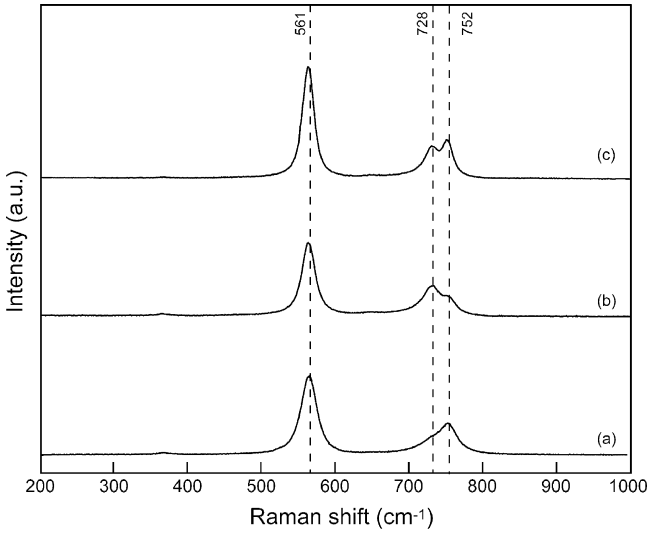

Fig. 3. Raman shift spectra of IrO_2 thin films deposited at $P_{O_2} = 20$ Pa and (a) $T_{sub} = 573$ K, (b) 673 K and (c) 773 K.

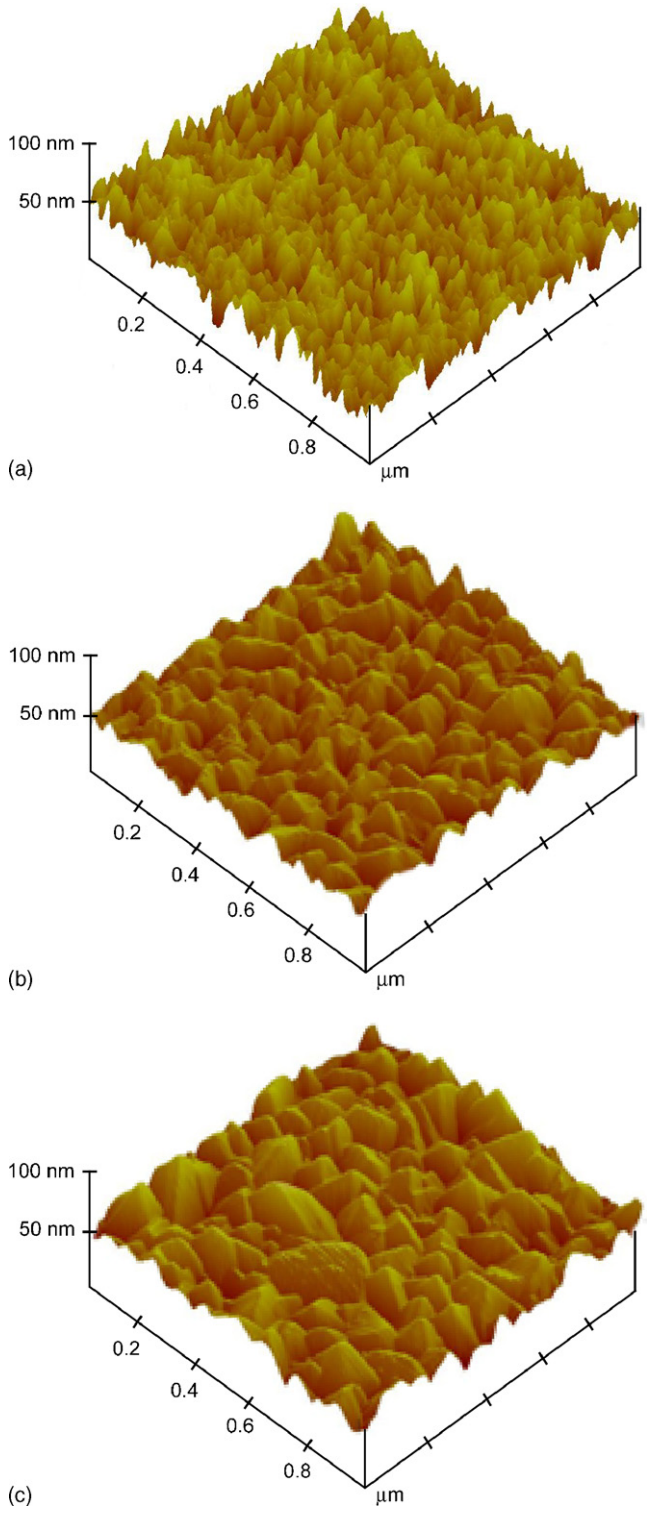

Fig. 4. Three-dimensional tapping mode AFM images of the surface morphology of IrO_2 thin films prepared at $P_{O_2} = 20$ Pa and (a) $T_{sub} = 573$ K, (b) 673 K and (c) 773 K.

[11], marked by dashed lines in the spectra. Good agreement between the observed and standard Raman peaks confirmed that the as-grown films were in pure IrO_2 phase, which was consistent with the XRD results. On the other hand, the full width at half maximum (FWHM) for the main peaks at

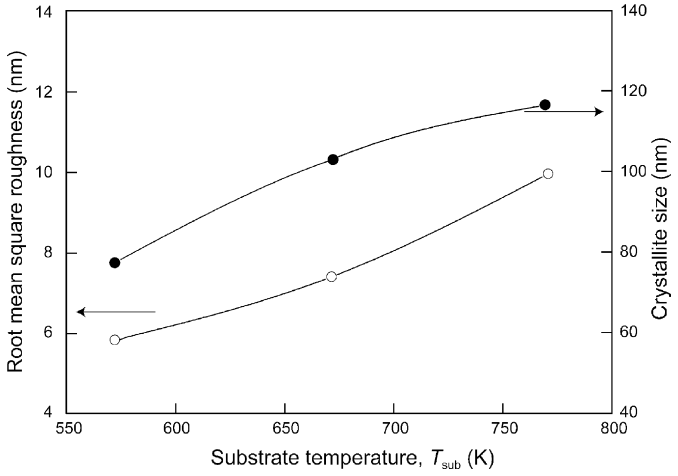

Fig. 5. Crystallite size and root mean square roughness of IrO_2 thin films as a function of T_{sub}.

561 cm^{-1} was about 16 cm^{-1}, similar to that of single crystalline IrO_2 (12 cm^{-1}). Such narrow peaks suggested a high degree of crystallinity. However, IrO_2 thin films exhibited slight red shifts, which could be due to the tensile stresses caused by the lattice mismatch between the films and substrates [12].

3.2. Surface morphology

Fig. 4 shows the three-dimensional tapping mode AFM images of the surface morphology of IrO_2 thin films prepared at $P_{O_2} = 20$ Pa and $T_{sub} = 573$–773 K. The crystallite size and root mean square roughness (RMS) of the films as a function of T_{sub} is illustrated in Fig. 5. Here, the average crystallite size was calculated from slow XRD scans (with steps of $2\theta = 0.02^\circ$ at 6 s/step) between 27° and 29° by using Scherrer's formula:

$$D = \frac{0.9\lambda}{\beta \cos\theta} \quad (2)$$

where D is the crystalline size of IrO_2 thin films, λ the wavelength of X-rays (0.15406 nm), β the full width at half maximum for (1 1 0) peak, and θ is the diffraction angle.

It can be seen from the figures that IrO_2 thin films deposited at $T_{sub} = 573$–773 K were well crystallized with a nearly dense texture. The average crystallite size of IrO_2 thin films changed with T_{sub}, varying from 77 nm at $T_{sub} = 573$ K to 103 nm at $T_{sub} = 673$ K and 116 nm at $T_{sub} = 773$ K. The increase in crystallite size resulted from the enhancement of film surface atomic mobility with the increasing of T_{sub}, which enabled the thermodynamically favored grains to grow [13]. The variation of roughness with T_{sub} was similar to that of crystallite size. The RMS values of IrO_2 thin films changed from 5.9 nm for $T_{sub} = 573$ K to 9.8 nm for $T_{sub} = 773$ K, showing a nearly smooth surface.

3.3. Electrical resistivity

Fig. 6 shows the room-temperature electrical resistivity of IrO_2 thin films deposited at $P_{O_2} = 20$ Pa and $T_{sub} = 573$–773 K.

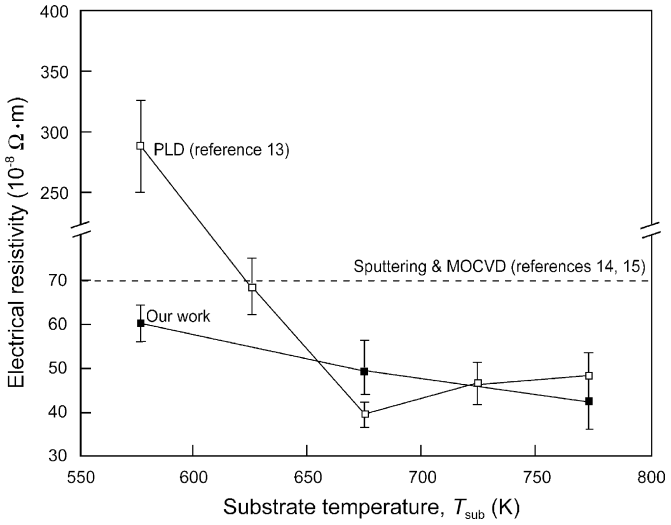

Fig. 6. Room-temperature electrical resistivity of IrO_2 thin films deposited at $P_{O_2} = 20$ Pa and $T_{sub} = 573$–773 K.

The resistivity values reported in literatures [13–15] were also depicted for comparison. It had been reported that IrO_2 films prepared by metal-organic chemical vapor deposition (MOCVD) at 623–723 K had the electrical resistivity of (70–730) $\times 10^{-8}$ Ω m [14]. The electrical resistivity of IrO_2 films with a (1 1 0) orientation, which were prepared by reactive sputtering, was about 70×10^{-8} Ω m [15]. IrO_2 thin films prepared by pulsed laser deposition (PLD) at $T_{sub} = 673$ K had the electrical resistivity of 39×10^{-8} Ω m [13], where Si(1 0 0) substrates were subjected to in situ oxidation prior to the deposition. According to our work, the electrical resistivity of the laser-ablated IrO_2 thin films decreased with T_{sub}, from $(60 \pm 3) \times 10^{-8}$ Ω m ($T_{sub} = 573$ K) to $(42 \pm 6) \times 10^{-8}$ Ω m ($T_{sub} = 773$ K) which was almost the same values as those of (0 1 1) and (0 0 1) oriented bulk single-crystalline IrO_2 (34.9×10^{-8} and 49.1×10^{-8} Ω m, respectively) [16]. Therefore, the resistivity values were relatively smaller, indicating that the laser-ablated IrO_2 thin films were highly conductive.

The resistivity variation of the laser-ablated IrO_2 thin films as a function of T_{sub} was mainly dependant on the changes in crystal orientation and surface morphology for difference T_{sub}. On the one hand, the preferred orientation of IrO_2 thin films changed into (1 0 1) at a higher T_{sub} of 773 K, while (1 0 1) oriented IrO_2 phase showed a lower electrical resistivity [13]. On the other hand, with the increasing of T_{sub} especially higher than 650 K, IrO_2 grains were more crystallized and the shapes changed gradually from the faceted to the rounded, which improved the interconnectivity between grains. As a result, the electrical resistivity of the laser-ablated IrO_2 thin films decreased with T_{sub} just as shown in Fig. 6.

4. Conclusions

Well crystallized IrO_2 thin films were prepared on Si(1 0 0) substrates by laser ablation at substrate temperatures (T_{sub}) from 573 to 773 K and in an oxygen partial pressure of 20 Pa. The preferred orientation of the laser-ablated IrO_2 thin films changed from (2 0 0) to (1 1 0) and (1 0 1) depending on T_{sub}. With the increasing of T_{sub}, both the surface roughness and crystallite size of the films increased. The room-temperature electrical resistivity of IrO_2 thin films decreased with increasing T_{sub}, showing a low value of $(42 \pm 6) \times 10^{-8}$ Ω m at $T_{sub} = 773$ K. The resistivity variation as a function of T_{sub} was correlated with the changes in crystal orientation and surface morphology of the laser-ablated IrO_2 thin films.

Acknowledgements

This work is financially supported by Doctoral Research Fund of Wuhan University of Technology (451-35100149) and Key Fund of National Cooperation of Hubei Province.

References

[1] C.U. Pinnow, I. Kasho, N. Nagel, T. Mikolajick, C. Dehm, J. Appl. Phys. 91 (2002) 1707.
[2] R.K. Kawar, P.S. Chigare, P.S. Patil, Appl. Surf. Sci. 206 (2003) 90.
[3] K.G. Kreider, M.J. Tarlov, J.P. Cline, Sens. Actuators B: Chem. 28 (1995) 167.
[4] A.M. Serventi, M.A. ElKhakani, R.G. Saint-Jacques, J. Mater. Res. 16 (2001) 2336.
[5] T. Pauporté, D. Aberdam, J.-L. Hazemann, R. Faure, R. Durand, J. Electroanal. Chem. 465 (1999) 88.
[6] K. Nishio, Y. Watanabe, T. Tsuchiya, Thin Solid Films 350 (1999) 96.
[7] B.R. Chalamala, Y. Wei, R.H. Reuss, Appl. Phys. Lett. 74 (1999) 1394.
[8] M.A. El Khakani, M. Chaker, E. Gat, Appl. Phys. Lett. 69 (1996) 2027.
[9] Y.X. Liu, H. Masumoto, T. Goto, Mater. Trans. 45 (2004) 900.
[10] P.S. Patil, P.S. Chigare, S.B. Sadale, T. Seth, D.P. Amalnerkar, R.K. Kawar, Mater. Chem. Phys. 80 (2003) 667.
[11] P.C. Liao, C.S. Chen, W.S. Ho, Y.S. Huang, K.K. Tiong, Thin Solid Films 301 (1997) 7.
[12] M.S. Chen, Z.X. Chen, S.H. Tang, W.S. Shi, D.F. Cui, Z.H. Chen, J. Phys.: Condens. Matter 12 (2000) 7013.
[13] M.A. ElKhakani, M. Chaker, Thin Solid Films 335 (1998) 6.
[14] P.C. Liao, Y.S. Huang, K.K. Tiong, J. Alloys Compd. 317–318 (2001) 98.
[15] R.H. Horng, D.S. Wuu, L.H. Wu, M.K. Lee, Thin Solid Films 373 (2000) 231.
[16] W.D. Ryden, A.W. Lawson, C.C. Sartain, Phys. Rev. B 1 (1970) 1494.